CHAPTER

Geometrical Control of Actin Assembly and Contractility

2

Anne-Cécile Reymann, Christophe Guérin, Manuel Théry, Laurent Blanchoin, and Rajaa Boujemaa-Paterski

Laboratoire de Physiologie Cellulaire et Végétale, Institut de Recherches en Technologies et Sciences pour le Vivant, iRTSV, CNRS/CEA/INRA/UJF, Grenoble, France

CHAPTER OUTLINE

Abstract

The actin cytoskeleton is a fundamental player in many cellular processes. Ultrastructural studies have revealed its extremely complex organization, where actin filaments self-organize into defined and specialized structures of distinct functions and, yet, are able to selectively recruit biochemical regulators that are available in the

Methods in Cell Biology, Volume 120 **ISSN 0091-679X**

http://dx.doi.org/10.1016/B978-0-12-417136-7.00002-1

entire cell volume. To overcome this extraordinary complexity, simplified reconstituted systems significantly improve our understanding of actin dynamics and self-organization. However, little is known regarding physical rules governing actin networks organization and to which extent network structure may direct and regulate selective interactions with specific regulators. Here, we describe the first method to direct actin filament assembly to specific 2D motifs with a finely tuned geometry and relative distribution. This method enables the study of how geometrical confinement governs actin network structural organization and how, in return, structural cues can control selective contraction by myosin motor. The protocol relies on the use of surface micropatterning and functionalization procedures in order to selectively direct actin filament assembly to specific sites of nucleation.

INTRODUCTION

Actin is a major cell component and the actin cytoskeleton is fundamental for many cellular processes ranging from morphogenesis to cellular motility (Pollard & Borisy, 2003). The actin network in cells displays distinct architectures specialized for well-defined functions. These architectures can be divided into three main classes. (i) A branched entangled and dense actin network localized underneath the plasma membrane, generating protrusive force production (Svitkina & Borisy, 1999; Urban, Jacob, Nemethova, Resch, & Small, 2010; Vinzenz et al., 2012; Weichsel, Urban, Small, & Schwarz, 2012). (ii) Antiparallel actin bundles running across the cell cytoplasm. These are contractile structures hosting myosin molecular motors and linked to the plasma membrane via focal adhesions (Gardel et al., 2008; Hotulainen & Lappalainen, 2006; Naumanen, Lappalainen, & Hotulainen, 2008; Takeya, Taniguchi, Narumiya, & Sumimoto, 2008; Vicente-Manzanares, Ma, Adelstein, & Horwitz, 2009). (iii) Parallel actin bundles are present in the dorsal area of cells and in the "linear protrusions" of the plasma membrane called filopodia (Nicholson-Dykstra & Higgs, 2008; Yang & Svitkina, 2011). They are not contractile structures (Block et al., 2008; Hotulainen et al., 2009; Mattila & Lappalainen, 2008; Schirenbeck, Bretschneider, Arasada, Schleicher, & Faix, 2005; Steffen et al., 2006; Yang et al., 2007). All these specialized actin structures overlap within the cell volume and are controlled by more than 70 regulatory protein families (Pollard & Borisy, 2003). However due the extraordinary cellular complexity (Xu, Babcock, & Zhuang, 2012), it is difficult to study in detail and decouple the biochemical and physical laws that govern the dynamics of actin networks. During the past decades, *in vitro* simplified reconstituted systems, in bulk solution (Pollard & Borisy, 2003) or using pathogens and functionalized particles (Cameron, Footer, Van Oudenaarden, & Theriot, 1999; Frishknecht et al., 1999; Giardini, Fletcher, & Theriot, 2003; Loisel, Boujemaa, Pantaloni, & Carlier, 1999; Noireaux et al., 2000; Pantaloni, Boujemaa, Didry, Gounon, & Carlier, 2000; Reymann et al., 2011; Romero et al., 2004) overcame the cell complexity

and significantly improved our understanding of actin dynamics. Unfortunately, these reconstituted systems were unable to investigate to which extent geometrical confinement may be a determinant for actin network self-organization into specific architectures.

In vivo studies have reported that actin substructures are often associated with a specific cortege of regulatory factors, which are yet available in the entire cell volume. Even if it is now well established that the recruitment of many actin regulators is under tight biochemical control including the nucleotide state of actin subunits or the exclusive interactions of some actin regulators (Pollard & Borisy, 2003), the extent to which network structural organization plays a role in these selective interactions is still unclear. More specifically, recent cell studies reported the crucial role of myosin in actin network turnover during cell motility. Although the motor protein is available in the entire cell, myosin had been shown to localize, contract and disassemble specific actin substructures (Burnette et al., 2011; Vallotton, Gupton, Waterman-Storer, & Danuser, 2004; Wilson et al., 2010). Therefore, further investigations remain to be carried out to shed light on the biochemical or physical factors controlling selective recruitment of regulators on defined actin organizations.

Here, we describe the first method to assemble structured actin networks on micropatterns and analyze how geometrical confinement governs actin network organization (Reymann et al., 2010). Micropatterning allows grafting of nucleation promoting factors (NPFs) on a wide repertoire of geometries. These innovative biomimetic systems enable the reconstitution of branched, parallel, and antiparallel actin organizations observed in cells (Reymann et al., 2010). Furthermore, as micropatterning reconstitutes these three actin organizations separated in space, it interestingly permits the investigation of the extent geometrical actin filament organization can govern the selective recruitment of specific regulatory proteins. Here, we describe the method we used to assess myosin-induced selective contraction and the cross-linking by alpha-actinin of defined actin structures.

2.1 DEEP UV MICROPATTERNING METHOD: GEOMETRY RULES FOR ACTIN NETWORK ORGANIZATION

We present here a simple and straightforward method allowing the polymerization in a reproducible fashion of actin on micropatterned features. It consists in printing adhesive micropatterns on a uniformly repellent layer. These patterns are then selectively coated with NPFs triggering actin filament assembly while repellent areas remain bare of actin nucleation (Fig. 2.1). This protocol is an adapted version of a former one published by Azioune and collaborators describing in details the procedures used to micropattern glass surfaces for cell adhesion (Azioune, Storch, Bornens, Thery, & Piel, 2009). While keeping the same technique for the design of the chrome mask, we hereafter describe precisely a novel protocol specifically adapted to design functionalized micropatterned motifs required for actin polymerization *in vitro*.

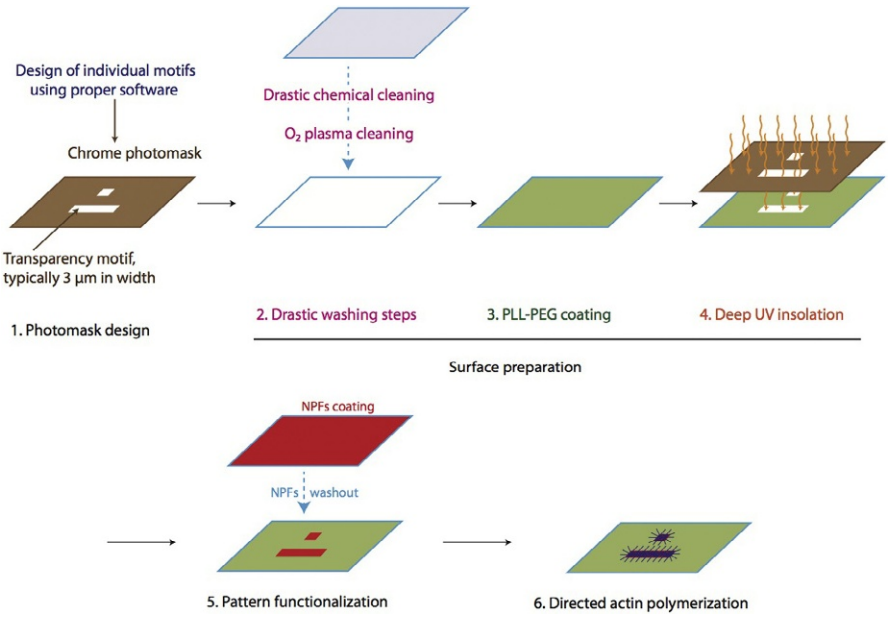

FIGURE 2.1

Overview of the protocol's main steps enabling directed polymerization of actin network on micropatterned surfaces. Each of the numbered steps is extensively described in the following sections, 2.1.1 to 2.1.3.

2.1.1 Designing the chrome mask and nucleation geometries

Photomasks. The creation of a proper photomask starts with some inventiveness and a careful design of individual motifs and their judicious juxtaposition. There are several software packages available on the market and any of them permitting a drawing with precise and clear indications of size will allow the mask producing company to convert the file into the proper format prior to its production. We use Clewin Software. For deep UV radiation, the photomask needs to be transparent to wavelengths below 200 nm. The material required for that is fused silica or synthetic quartz. The photomask has a specific resolution provided by the company that usually is around 1 µm. This resolution and the quality of the tight contact between the surface to pattern and the photomask during the UV radiation are two parameters that control the size of the features to be printed onto the photomask (Azioune et al., 2009). We typically draw features of 3 µm in width, which allows a remarkable size and shape reproducibility with accuracy.

Designing features. First of all, bear in mind that the choice of NPFs and experimental conditions are also to be taken into account while choosing the width of motifs. A large nucleation region will need several primer nucleation events to trigger the covering of the whole surface, such history could impact both the timing and homogeneity of the nucleation geometry as well as modifying the outcome network

(Achard et al., 2010). In opposite a very thin/small zone might not be very reproducibly covered.

Second, the surface area prone to actin nucleation (transparent zone) should not be designed too large, in order to avoid fast depletion of proteins and sinking of proteins in nonessential zones such as in surrounding localization grids (which, for example, are intentionally designed large for cell patterning). For the same reason, the distance between repeated motifs should be large enough. This distance should also take into account the length scale of potential actin filament growth in order to avoid one pattern influencing its neighboring ones. A distance of 100–800 μm is typically chosen.

Lastly, in order to easily repeat experiments in the exact same condition, it could be useful to design a set of horizontal repetition of motifs such as one could easily pattern identically several 20×20 mm coverslips.

2.1.2 Micropatterned surface preparation

1. Material
   - Glass coverslip purchased from Agar Scientific
   - Ethanol
   - MilliQ water
   - Hellmanex
   - Isopropanol
   - Parafilm
   - Adhesive double tape. We use a precut double tape 70 μm thick. It can be ordered from LIMA company, France
   - PLL-PEG purchased from CYTOO, Grenoble, France
   - PLL-PEG solution is prepared in Hepes 10 mM pH 7.4. An efficient coating of the glace surface with PLL-PEG needs plasma-cleaned surfaces but it also depends on the freshness of the PLL-PEG solution as well as the pH to be adjusted to 7.4
   - $10 \times$ KMEI buffer containing 500 mM KCl, 10 mM $MgCl_2$, 10 mM EGTA, and 100 mM imidazole, pH 7.0
   - Petri dishes (for storage of cleaned and passivated glass surfaces)
2. Equipment
   - Plasma cleaner, Plasma system Femto from Diener electronic company
   - UV ozone oven, UVO cleaner—ref. 342–200—from Jelight company
   - Vacuum mask holder; for detailed description refer to Azioune et al. (2009)
3. Methods

– Surface cleaning and PLL-PEG coating:

A quick and efficient means of passivating surfaces for micropatterning is to uniformly coat glass coverslips with PLL-PEG. Prior to that and in order to optimize the formation of a regular repellent layer of PEG chains, we perform a rigorous cleaning procedure of the glass surface, ensuring a total removal of dusts and fats.

THE PLASMA CLEANING:

In this paragraph, it is important to keep in mind that the washing steps in MilliQ water solution are crucial. They have to be performed with care and in extensive

volumes to ensure a total removal of any traces of chemicals that may persist on the glass surface and interfere either with the PLL-PEG coating or with the proteins present in the polymerization mixture.

1. The slides are washed with 100% ethanol and wiped with clean absorbent paper. Dried coverslips are then rinsed with MilliQ water and dried with a filtered airflow.
2. Load the slides in a suitable slide holder and sonicate them in acetone for 30 min at room temperature.
3. Transfer the slides to an ethanol solution and incubate for 10 min at room temperature. The slides are afterward washed extensively with MilliQ water.
4. Incubate the slides in a 2% Hellmanex III solution for 2 h at room temperature. The slides are afterward washed extensively with MilliQ water, dried with a filtered airflow and stored in a clear container at 4 °C.
5. Cleaned slides are then activated in O_2 plasma for 3 min at 80–90% of full power of 100 W.
6. Immediately afterward the activated slides should be incubated in PLL-PEG.

THE PLL-PEG COATING:

1. Dilute PLL-PEG powder (stock −20 °C) to 1 mg/ml in Hepes 10 mM pH 7.4 (store at +4 °C). Freshly dilute this 1 mg/ml solution before use to 0.1 mg/ml in Hepes 10 mM pH 7.4.
2. Immediately after being oxidized with O_2 plasma, incubate each coverslip with 100 µl of 0.1 mg/ml PLL-PEG solution (for 20 × 20 mm coverslips) on Parafilm for 30 min at room temperature. After introducing an additional 100 µl of Hepes 10 mM pH 7.4 between glass and Parafilm, delicately and slowly lift up the coverslip in order to allow a complete removal of the PLL-PEG solution. If the PLL-PEG coating was successful, the coverslip should come off perfectly dry with only one tiny droplet remaining at the very edge. Dry the remaining droplet softly with filtered airflow or carefully wipe it off with a nonabrasive tissue such as a Kimwipe (from Kimtech Science).
3. Store PLL-PEG-coated coverslips in petri dishes in the fridge for up to 2 weeks. We seal the petri dishes with a plastic film such as Parafilm to avoid dust and desiccation.
   – Surface patterning and functionalization

UV patterning is performed the same day as the actin polymerization assay. We indeed found that coating the adhesive patterns with NPFs just after the UV insolation improves the efficiency of this step. The patterned areas are therefore uniformly coated and the actin polymerization starts promptly. The next steps are to be carried out in the following order:

1. Wash the chrome mask successively with MilliQ water and isopropanol, and dry it with a filtered airflow. The chrome mask surface to be applied on the PLL-PEG-coated side of the coverslip must be free of any impurity in order to ensure a tight contact.

2. While preheating the UV oven for 2 min, or as it is recommended in the manufacture's instructions, gently clean both sides of the PLL-PEG-coated coverslips with a filtered airflow and the vacuum mask holder to ensure complete removal of dust. Preheating the oven ensures the irradiation to be reproducibly performed at the same constant power.
3. Place the coverslip with its PLL-PEG-coated side facing upwards. Carefully place the chrome mask over it. In order to obtain well-defined micropatterns (of at least 3 μm in width), during deep UV radiation the mask must be maintained in tight contact with the coverslip. The vacuum mask holder allows tight contact only when the mask is well balanced on the holder. To do so we use supplementary cleaned, dried and noncoated coverslips evenly positioned throughout the surface.
4. Then UV irradiate through the chrome mask for 5 min.
5. Immediately after UV patterning, incubate the patterned surfaces with the NPFs solution. We incubate each 20×20 mm coverslip with 30 μl pWA at a final concentration of 1 μM for 15 min on Parafilm sheet at room temperature. Each coverslip is then gently washed for 30 s in a small Petri dish in a large volume of $1\times$ KMEI buffer (10 ml). When delicately lifted out the coverslip should be already dry on the PLL-PEG surface, if needed dry the other surface with a Kimtech tissue. You can then store for 48 h these coated pWA coverslips in a clean box at 4 °C before use.

2.1.3 Polymerization of structured actin filament network on Micropatterned surfaces

1. Material
   - Methylcellulose (1500 cP), Sigma M0387, prepared at 2% in MilliQ water solution.
   - BSA, Sigma A7030, resuspended in MilliQ water solution to make a 10% (w/v) and stored at −20 °C.
   - Buffers adapted to actin polymerization on micropatterns:
     1. *Fluorescence buffer*. Prior to actin polymerization on pWA-coated micropatterns, a fluorescence buffer is freshly prepared to provide the medium with an enzyme system to antagonize free radical formation that causes photodamage. This buffer contains 15 mM imidazole, pH 7.0, 74 mM KCl, 1.5 mM $MgCl_2$, 165 mM DTT, 2 mM ATP, 50 μM $CaCl_2$, 5 mM glucose, 30 μg/ml catalase, 155 μg/ml glucose oxidase, and 0.75% methylcellulose.
     2. *10× KMEI buffer*. It contains 500 mM KCl, 10 mM $MgCl_2$, 10 mM EGTA, and 100 mM imidazole, pH 7.0.
   - Valap soft wax is made of equal parts, by weight, of Vaseline, Lanolin, and Parafin wax. These three components can be purchased from Fisher/VWR. Valap is maintained molten in a container on heater block at a temperature of 50–55 °C. As Valap wax is a biologically inert material, use this solution

rather than nail polish for sealing coverslips to avoid evaporation during imaging of actin polymerization.

2. Equipment
   - A flow cell chamber
     - Wash the glass slide with water and ethanol just before use.
     - Assemble a flow cell using a clean glass slide, a pWA-coated coverslip, and precut adhesive double tape 70 μm thick (Fig. 2.2).
   - A dry block heater can be purchased from VWR, if Valap soft wax is used to seal the flow cell chamber.
   - Epifluorescence microscope. Images can be taken using an upright BX61 Olympus microscope equipped with a 40× dry objective (UPLFLN, NAD0.75), a computer controlled fluorescence microscope light source *X-Cite 120PC Q*, a motorized XY stage (Marzhauser, Germany) and a CoolSnap HQ2 camera (Roper Scientific, Germany). The microscope and

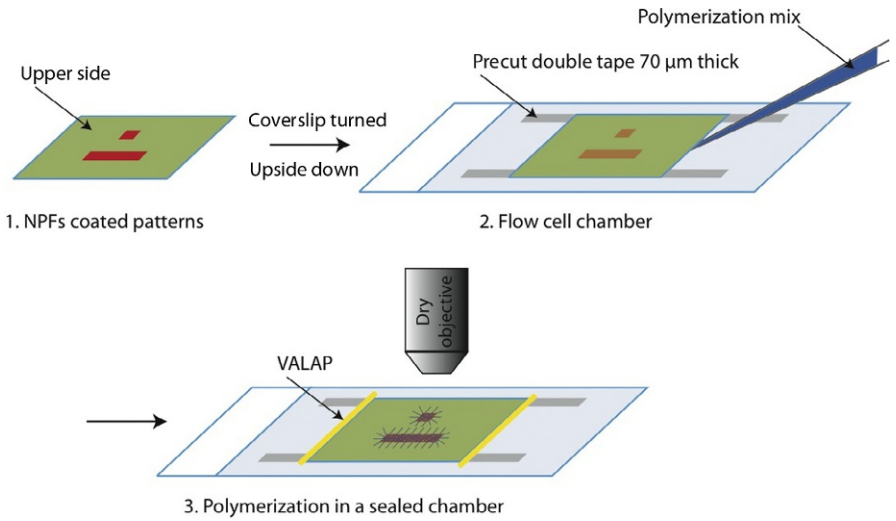

FIGURE 2.2

Actin polymerization is reconstituted in a flow cell chamber. The 20 × 20 mm NPFs-coated coverslip is turned upside down on top of a cleaned glass slide using precut adhesive tapes (70 μm thick) as spacers for the chamber. Freshly assembled polymerization mix is injected, the chamber is sealed with VALAP soft wax, and actin dynamics is followed with epifluorescence microscopy. A dry objective is useful when several positions are observed simultaneously as it prevents pressure-driven flow within the flow cell that may damage the reconstituted actin filament structures during XY stage movements.

devices are driven by MetaMorph (Molecular Devices, Downington, PA). The use of the motorized stage is extremely useful as it allows reproducibility to be assessed by acquiring actin dynamics on multiple identical micropatterns under exactly the same biochemical conditions.

3. Methods
   1. Prepare all buffers and protein dilutions
   2. Mix the following ingredients, respecting the order:
      - 3 µl 10× KMEI
      - 2 µl BSA 10%
      - (*X* µl) compensation with G buffer to 30 µl total volume
      - 6 µM Profilin (three times the monomeric actin concentration)
      - 50–150 nM Arp2/3 complex
      - 10 µl fluorescence buffer
      - 2 µM actin monomers, 7% labeled with Alexa fluorophore to enable visualization of polymerizing actin filament networks using epifluorescence microscopy
      - homogenize this polymerization mix extremely carefully before introducing it in the flow cell. This is a crucial step as the presence of methylcellulose in the solution may induce inhomogeneity in the motility medium that may bias the results
      - Seal flow cell with melted VALAP
   3. Observation of actin polymerization

      If using an automated microscope equipped with a motorized stage to follow actin network assembly, 20–30 positions are first recorded before acquiring their subsequent time lapses. The Multi-Dimensional Acquisition plugin of the MetaMorph software, which drives our microscope and optical devices, easily allows such sequential acquisition. To reduce the photodamage generated on actin filaments due to repetitive illuminations, the light source is set to 12 or 20% of its maximal power, the exposure time to 50 ms, and one image is taken every 2–3 min for around 30 min to 1 h, the time necessary to reach the steady state of actin polymerization. It is also judicious to use an automated correction of the focus (such as perfect focus or the software's inbuilt auto focusing tool) for long-term observation.

In an optimal experiment one should be able to distinguish nucleation on the patterns from the background fluorescence after a few minutes, and the final contrast between geometrically constrained networks and free filaments in the medium should be so that one should not distinguish the later in a nonsaturated image. What is important is that the few filaments in the medium should not influence the growing structures on patterns. The main challenge that one encounters while doing such experiment is to find a good equilibrium between spontaneous nucleation, necessary to initiate a primer nucleation event within all NPFs areas (Achard et al., 2010) and proper nucleation triggered on the surface of patterns.

In the case of Arp2/3 complex-promoted nucleation, polymerization on the patterns should be dense and constitutes an entangled meshwork of branched filaments on all patterns. Playing with geometry, actin filaments grown on patterns can then be selectively organized in parallel, antiparallel, and cross-linked fashion. For further details refer to Nature Material, Reymann et al., 2010.

2.2 STRUCTURED NETWORK ASSEMBLY IN THE PRESENCE OF CROSS-LINKERS

Numerous actin cross-linkers, such as fascin or alpha-actinin, while added to actin polymerization mix can be used to increase the persistence length of filaments and modify the geometrical arrangement of growing networks (Gardel et al., 2004; Haviv et al., 2006; Svitkina et al., 2003; Vignjevic et al., 2003; Wagner, Tharmann, Haase, Fischer, & Bausch, 2006). Be aware that such additional proteins may impact also the initial nucleation step as well as generating more abundant outside-pattern perturbing structures. For this reason, two experimental procedures can be compared and chosen accordingly to the addressed question: either cross-linkers can be added directly to the other proteins, before introduction of the polymerization mix in the flow cell, or once nucleation and polymerization on patterns are started in droplet.

2.2.1 Addition of Cross-Linkers at the onset of actin assembly

The implemented polymerization mix can be assembled as mentioned in the section above and the required amount of the cross-linker can be introduced just before adding the fluorescence buffer.

2.2.2 Addition of Cross-Linkers at steady state of actin assembly

This procedure is much more delicate to achieve because the smallest flow will affect and modify the self-induced actin network organization. In order to avoid such artifacts, a small volume containing cross-linker can be added on top of a larger droplet including the initial nucleation mix sitting on the top of the micropattern coverslip. The local introduction of proteins inevitably leads to the formation of a protein gradient instead of a uniform concentration throughout the sample. Moreover, such open configuration needs to be kept in humid chamber also during recording under the microscope in order to avoid fast evaporation.

Furthermore, the observation of actin polymerization on micropatterns in the droplet open medium needs the use of an inverted microscope. We use a TE2000-E Nikon microscope equipped with a 1006 CFI Plan Fluor oil objective or 606 CFI Apo TIRF oil objective (MRH02900 and MBH76162, respectively, Nikon), a motorized XY stage (Marzhauser), and a QUANTEM:512SC cooled EMCCD camera (Photometrics). The microscope and devices are driven by MetaMorph (Molecular Devices, Downington, PA). As we mentioned above, the use

of a motorized stage is judicious in assessing reproducibility of actin dynamics on micropatterns.

2.3 STRUCTURED NETWORK ASSEMBLY IN THE PRESENCE OF MYOSIN MOLECULAR MOTOR

Molecular motors such as myosins are abundantly found embedded in actin networks within different cellular structures. Their ability to produce forces can induce an accumulation of stress and shear within the underlying actin network that can lead to its deformation, contraction and disassembly or simply allow processive motors to walk along actin tracks. Different aspects of such phenomenon can be studied on micropattern structures. In this section, we will first concentrate on the case where molecular motors are localized and fixed to designed positions. In the last part of this section, we will discuss how to reconstitute structured actin network contraction and disassembly driven by interacting motor myosins freely available in solution, case which falls back very close to the previous topic of additional cross-linkers discussed in Section 2.2.

2.3.1 Second surface patterning

Grafting molecular motors onto micropatterns can be achieved after the preparation of a first set of patterns coated with NPFs (Section 2.1). This allows the study of interactions between controlled actin architectures and localized molecular motors, reproducing what could happen *in vivo* at focal adhesion sites, for example, or enabling an easier study of force production/response as the sites of nucleation and force production are decoupled and could be geometrically controlled. For the generation of a second set of patterns two options are possible. The first is to use a second round of UV-based micropatterning through a chrome mask, this allows very simply and very fast the creation of numerous new motifs superimposed over the first set of motifs. The drawback often being that you cannot control the alignment of both sets if you do not have a mean of precisely aligning the chrome mask. The second option is to use live laser patterning to design the second set of patterns (Vignaud et al., 2012). This option allows very precise control of the juxtaposition between the two kinds of patterns, with the only drawback being that it is more time consuming.

In the protocol described hereafter, myosin is not directly attached to glass/micropatterned surface, but through protein G–antibody conjugates. These linkers allow a more homogenous and reproducible coating of active myosin while avoiding myosin heads from becoming stuck to the surface. Coating of molecular motors directly on the micropatterns is also possible though (Fig. 2.3).

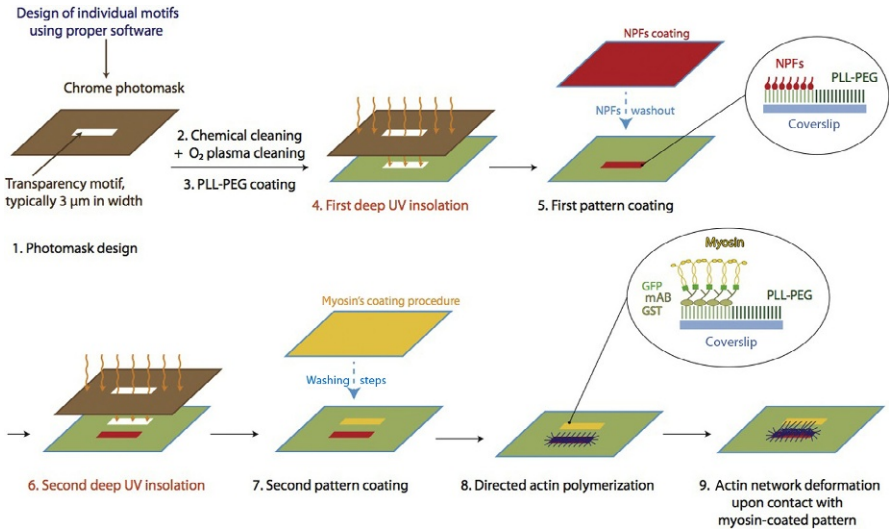

FIGURE 2.3

Actin polymerization is reconstituted in a flow cell chamber in the presence of grafted myosin. The 20×20 mm NPFs-coated coverslip is directly used for a second round of deep UV patterning in order to print new micropatterns dozens of micrometers apart from the former ones. This second generation of patterns is then grafted with fluorescently labeled myosin through protein G–antibody auxiliaries (as precisely described in the following sections). The double-patterned coverslip is then used to assess the interaction (recruitment, traction, and eventually deformation) between actin filament networks polymerized on NPFs-coated patterns and the neighboring grafted myosins.

1. Materials
   - NPF-coated micropatterns coverslips prepared as explained in Section 2.1.
2. Equipment
   - The Plasma cleaner, Plasma system Femto from Diener electronic company.
   - UV ozone oven, UVO cleaner—ref. 342–200—from Jelight company.
   - Vacuum mask holder; for detailed description refer to Azioune et al. 2009.
3. Methods
   1. Once the coating of the first set of micropatterns has been completed with NPFs as described in Section 2.1, very gently let the surface dry and if needed store at 4 °C.
   2. For the second surface-patterning step, proceed as explained in Section 2.1, paragraph "Surface patterning and functionalization," steps 1–4. More precisely, we directly use the freshly prepared NPFs-coated coverslips for a second round of deep UV exposure through the photomask. Immediately afterward, use the double-patterned coverslip to mount a flow cell chamber and graft myosin as described below (Fig. 2.3).

Tips for succeeding in juxtaposing the first and second set of micropatterns: One can easily mark position and orientation of the coverslip with respect to the

photomask during the first round of UV irradiation. For actin filaments to reach and be recruited by grafted myosins, the myosin-coated micropatterns should be 20–50 μm apart from the nucleation ones. Therefore, for the second round of exposure to UV, placing the coverslip in its former position allows the microscopic shift required between the two sets of micropatterns.

2.3.2 Myosin grafting

1. Materials
   - Myosin, eventually GFP-labeled, should be diluted at the last minute in M-buffer to the desired concentration and stored concentrated at −20 °C in 50% glycerol.
   - Protein G (Sigma 19459), diluted to 1 M in water containing 10 mM Imidazole pH 7.5. Protein G is a small globular cell surface protein produced by *Streptococcus* sp. It comprises specific domains that bind with high affinity to the constant Fc region of most mammalian immunoglobulins (IgGs) (Sauer-Eriksson, Kleywegt, Uhlen, & Jones, 1995).
   - Mouse monoclonal antibody raised against full length recombinant GFP, targeting the GFP–myosin construct and binding to protein G (isotype: IgG2a), Tebu MAB4183, diluted in filtered TBS to a final concentration of 0.2–0.5 mg/ml.
   - BSA, Sigma A7030, resuspended in MilliQ water solution to make a 10% (w/v), aliquoted and stored at −20 °C.
   - Unlabeled monomeric actin
   - Buffers adapted to myosin
     1. 20× TBS buffer contains 20 mM Tris–HCl pH 7.5, 150 mM NaCl and to be freshly diluted to 1× before use
     2. 10× KEEI buffer contains 800 mM KCl, 0.1 mM EDTA, 10 mM EGTA, 100 mM Imidazole, and adjusted to pH 7.
     3. M-Buffer contains 1× KEEI, 5 mM ATP, 5 mM $MgCl_2$, 2 mM DTT
2. Equipment
   - Humid clean chamber on ice
3. Methods
   1. Mount the double-patterned coverslip in flow cell chamber as described in Section 2.1, and from now on place in humid chamber kept on ice.
   2. Protein G incubation: introduce 30 μl of 0.5 mg/ml for 30 min; wash with three times 200 μl TBS.
   3. Antibodies incubation: introduce 30 μl of 100–200 μg/ml for 60 min, wash with three times 200 μl TBS.
   4. BSA incubation: introduce 5% BSA for 15 min, wash with 200 μl TBS.
   5. Myosin incubation: incubation of 30 μl of myosin diluted in M-buffer at 80 nM between 30 and 60 min, wash with 200 μl M-buffer.
   6. Black actin incubation: introduce 30 μl of G-actin diluted in M-buffer for 5 min. Wash with 200 μl of M-buffer. This step saturates eventual dead myosin heads with unlabeled actin and avoids potential nondynamic capture of future growing actin filaments.
   7. Proceed without delay to actin polymerization and observation.

2.3.3 Actin polymerization in the presence of grafted myosins

Decoupling the sites of nucleation and force production allowed us to verify the directional motion of myosin motor (Reymann et al., 2012), and probe to what extent entanglement between adjacent branched networks is stable (Fig. 2.4). For such purpose the simplest geometry consists of two sets of parallel bars. The first set contains bars spaced apart with a variable distance and coated with NPFs. While the second surface-patterning set of bars, interdigitated with the first ones, is coated with myosins. NPFs-coated bars generate a dense actin network from which escape actin filaments oriented with their barbed ends growing outward and organized into a parallel actin structure. They are able to grow long enough to reach the neighboring myosin-coated bar and be recruited by the immobilized motors (Fig. 2.4). Depending on the polarity of myosin motion these incoming barbed ends can either be pushed

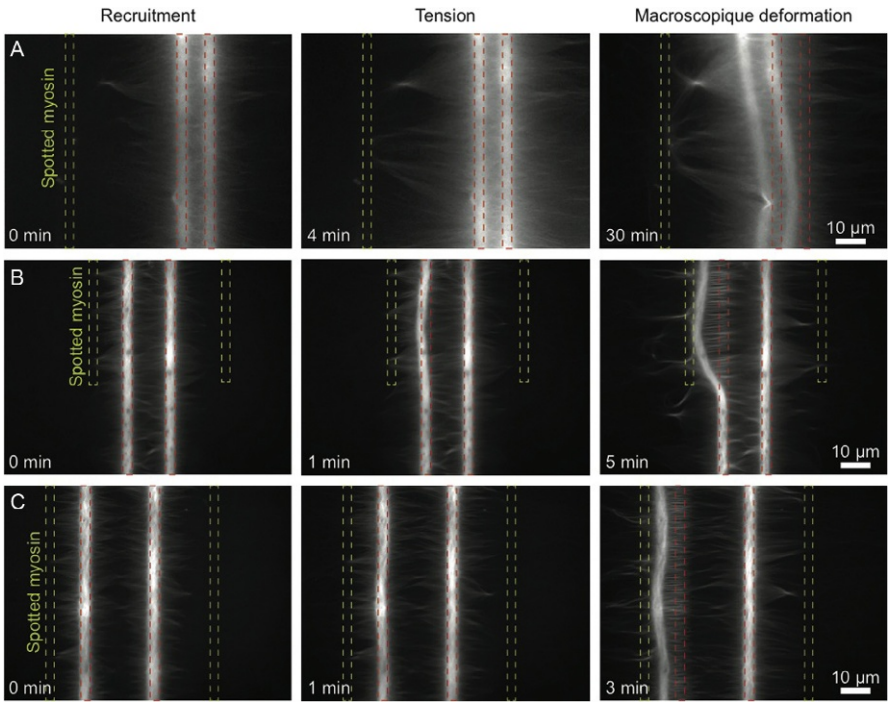

FIGURE 2.4

Myosin-induced deformation of entangled actin networks. Epifluorescence microscopy is used to follow actin polymerization on NPFs-coated bars adjacent to myosin-coated ones. Nucleation bars were spaced with 6 µm (A), 12 µm (B), and 24 µm (C). The reconstituted medium composition is extensively described in Section 2.3. As the distance between two nucleation bars increased, the interaction forces existing between the two adjacent actin networks were not able to resist myosin-induced traction force.

and buckled or be pulled (Reymann et al., 2012). In the case of pulling, the traction force applied by surface-bound myosins to the incoming array of filaments is transmitted to its entangled mother network and can be sufficient to deform and detach it from the NPFs-coated pattern. If such a network is connected to an adjacent nucleating network, the global structure is also subjected to traction forces leading to its macroscopic deformation (Fig. 2.4A). However, if the two networks are further apart, only the network that is closest to the motor myosin is deformed (Fig. 2.4B and C). Our results clearly demonstrated that the larger the distance between nucleation bars, the less stable is the connection between the two networks (Fig. 2.4). We believe that such cohesion resides in the history of nucleation and growths of both structures. When a small distance separates two nucleation bars, actin filaments elongating outwards are short when they reach the adjacent network. Therefore, they are stiff enough to elongate through the dense actin array of parallel filaments and reach the nucleation region where they are likely to initiate new branched networks, thereby increasing connectivity and strengthening cohesion between networks initiated on two adjacent bars (Reymann et al., 2010). In contrast, when nucleation bars are spaced apart with larger distances, filaments forming the antiparallel organization are longer, more flexible and therefore unable to reach the adjacent nucleation site and ensure stronger entanglement (Fig. 2.4).

1. Materials
   - ATP regeneration system
     Pyruvate Kinase from Rabbit muscle (Sigma P9136-5KU)-PK, diluted to 10^5 U/ml in 50% glycerol and stored in −20 °C.
     Phospho(enol)pyruvic acid monopotassium salt (Sigma P7127-100 mg)—PEP, dilution to 100 mM (or 103 mg for 5 ml), pH adjusted to 7.5 with NaOH or HCl and stored at −20 °C. The stock solution can be frozen and thawed several times.
   - Fluorescence buffer (as described in Section 2.1)
2. Equipment
   - A flow cell chamber
     - Wash the glass slide with water and ethanol just before use.
     - Assemble a flow cell using a clean glass slide, a double micropatterned coverslip coated with pWA and myosin, and precut adhesive double tape 70 µm thick (Fig. 2.2).
   - A dry block heater can be purchased for VWR, if Valap soft wax is used to seal the flow cell chamber.
   - Epifluorescence upright microscope setup described in Section 2.1.
3. Methods
   1. Prepare all buffers and dilution of proteins
   2. Mix the following ingredients, respecting the order:
      – 3 µl 10× KMEI
      – (X µl) compensation with G buffer to 30 µl total volume
      – 2 µl BSA 10%

- 6 μM profilin (three times the monomeric actin concentration)
- 50–150 nM Arp2/3 complex
- 2 mM PEP
- 2000 U/ml PK
- 3 μl of Mg/ATP (extemporarily prepared: 10 μl ATP 0.1 M + 1 μl $MgCl_2$ 1 M + 39 μl H_2O)
- 10 μl fluorescence buffer
- 2 μM actin monomers 7% labelled with an Alexa fluorophore for instance.

3. Homogenize this polymerization mix before introducing it in the flow cell. Seal open edges with melted Valap (as described in Section 2.1)
4. Imaging (as described in Section 2.1)

2.3.4 Actin dynamics in the presence of myosin freely available in solution

The next step in understanding how myosins are selectively directed to specific actin substructures, while being available in the entire volume of cells, is to reconstitute actin networks driving selective contraction and disassembly induced by free myosin present in solution at the onset of actin polymerization on micropatterns. Therefore to assess how actin network architecture may control spatial and temporal recruitment of interacting motors, myosin is added directly to the polymerization mix in the presence of ATP regeneration system. Be aware that in this case the orientation, geometrical disposition, nature and density of actin structures are of upmost importance to drive and localize myosin distribution (e.g., parallel filaments will serve as unidirectional tracks for motion and dense meshwork will act as a trap) (Reymann et al., 2012).

1. Materials
   - ATP regeneration system (as described in Section 2.3.3)
   - Fluorescence buffer (as described in Section 2.1)
2. Equipment
   - A flow cell chamber
     - Wash the glass slide with water and ethanol just before use.
     - Assemble a flow cell using a clean glass slide, a pWA-coated coverslip, and precut adhesive double tape 70 μm thick (Fig. 2.2).
   - A dry block heater can be purchased for VWR, if Valap soft wax is used to seal the flow cell chamber.
   - Epifluorescence upright microscope setup described in Section 2.1.
3. Method
   1. Prepare all buffers and dilution of proteins
   2. Mix the following ingredients, respecting the order:
      - 3 μl 10 × KMEI
      - (*X* μl) compensation with G buffer to 30 μl total volume
      - 2 μl BSA 10%
      - 6 μM Profilin (three times the monomeric actin concentration)

- 50–150 nM Arp2/3 complex
- 2 mM PEP
- 2000 U/ml PK
- 3 µl of Mg/ATP (extemporarily prepared: 10 µl ATP 0.1 M + 1 µl $MgCl_2$ 1 M + 39 µl H_2O)
- 10 µl Fluorescence buffer
- the required concentration of myosin (diluted at the last minute: glycerol-myosin stock + required volume of M-buffer)
- 2 µM actin monomers 7% labelled with an Alexa fluorophore for instance.

3. Homogenize this polymerization mix before introducing it in the flow cell. Seal it with melted Valap (as described in Section 2.1)
4. Imaging (as described in Section 2.1)

CONCLUSION

Successful micropatterning of dynamic actin networks resides in the careful control of both surface preparation and biochemical conditions, such as nonpatterned surfaces remain bare of any "non-specific" actin assembly. We found that the use of profilin, as well as the quality and freshness of the black and labeled actin protein preparation, that must be exempt of any oligomers, helps to inhibit the spontaneous nucleation of actin filaments. Moreover, depending on the NPFs used to coat the patterned surfaces some adaptations in the chemical composition of buffers might be needed to ensure efficient binding. Therefore, even if we propose in this protocol a precise procedure for surface preparation, one has to find compromises to maximize directed NPFs binding and inhibition of spontaneous actin filament polymerization in solution that consumes monomers and competes with direct actin assembly on patterns.

Acknowledgments

This work was supported by grants from the Human Frontier Science Program (RGP0004/2011 awarded to L.B.), Agence Nationale de la Recherche (ANR-08-BLANC-0012 awarded to L.B.) and a PhD Fellowship from the IRTELIS program of the CEA (awarded to A.C.R.). We thank Enrique M. De La Cruz for myosin VI and V proteins, Cécile Sykes and Jan Faix for muscle myosin II protein, and James Sillibourne for insightful suggestions.

References

Achard, V., Martiel, J.-L., Michelot, A., Guérin, C., Reymann, A.-C., Blanchoin, L., et al. (2010). A "primer"-based mechanism underlies branched actin filament network formation and motility. *Current Biology*, *20*, 423–428.

Azioune, A., Storch, M., Bornens, M., Thery, M., & Piel, M. (2009). Simple and rapid process for single cell micro-patterning. *Lab on a Chip*, *9*, 1640–1642.

Block, J., Stradal, T. E., Hanisch, J., Geffers, R., Kostler, S. A., Urban, E., et al. (2008). Filopodia formation induced by active mDia2/Drf3. *Journal of Microscopy*, *231*, 506–517.

Burnette, D. T., Manley, S., Sengupta, P., Sougrat, R., Davidson, M. W., Kachar, B., et al. (2011). A role for actin arcs in the leading-edge advance of migrating cells. *Nature Cell Biology*, *13*, 371–381.

Cameron, L. A., Footer, M. J., Van Oudenaarden, A., & Theriot, J. A. (1999). Motility of ActA protein-coated microspheres driven by actin polymerization. *Proceedings of the National Academy of Sciences of the United States of America*, *96*, 4908–4913.

Frishknecht, F., Moreau, V., Röttger, S., Gonfloni, S., Reckmann, I., Superti-Furga, G., et al. (1999). Actin-based motility of vaccinia virus mimics tyrosine kinase signalling. *Nature*, *401*, 926–929.

Gardel, M. L., Sabass, B., Ji, L., Danuser, G., Schwarz, U. S., & Waterman, C. M. (2008). Traction stress in focal adhesions correlates biphasically with actin retrograde flow speed. *Journal of Cell Biology*, *183*(6), 999–1005.

Gardel, M. L., Shin, J. H., MacKintosh, F. C., Mahadevan, L., Matsudaira, P., & Weitz, D. A. (2004). Elastic behavior of cross-linked and bundled actin networks. *Science*, *304*, 1301–1305.

Giardini, P. A., Fletcher, D. A., & Theriot, J. A. (2003). Compression forces generated by actin comet tails on lipid vesicles. *Proceedings of the National Academy of Sciences of the United States of America*, *100*, 6493–6498.

Haviv, L., Brill-Karniely, Y., Mahaffy, R., Backouche, F., Ben-Shaul, A., Pollard, T. D., et al. (2006). Reconstitution of the transition from lamellipodium to filopodium in a membrane-free system. *Proceedings of the National Academy of Sciences of the United States of America*, *103*, 4906–4911.

Hotulainen, P., & Lappalainen, P. (2006). Stress fibers are generated by two distinct actin assembly mechanisms in motile cells. *Journal of Cell Biology*, *173*(3), 383–394.

Hotulainen, P., Llano, O., Smirnov, S., Tanhuanpää, K., Faix, J., Rivera, C., et al. (2009). Defining mechanisms of actin polymerization and depolymerization during dendritic spine morphogenesis. *Journal of Cell Biology*, *185*(2), 323–339.

Loisel, T. P., Boujemaa, R., Pantaloni, D., & Carlier, M.-F. (1999). Reconstitution of actin-based motility of Listeria and Shigella using pure proteins. *Nature*, *67*(53), 613–616.

Mattila, P. K., & Lappalainen, P. (2008). Filopodia: Molecular architecture and cellular functions. *Nature Reviews Molecular Cell Biology*, *9*, 446–454.

Naumanen, P., Lappalainen, P., & Hotulainen, P. (2008). Mechanisms of actin stress fibre assembly. *Journal of Microscopy*, *231*, 446–454.

Nicholson-Dykstra, S. M., & Higgs, H. N. (2008). Arp2 depletion inhibits sheet-like protrusions but not linear protrusions of fibroblasts and lymphocytes. *Cell Motility and the Cytoskeleton*, *65*, 904–922.

Noireaux, V., Golsteyn, R. M., Friederich, E., Prost, J., Antony, C., Louvard, D., et al. (2000). Growing an actin gel on spherical surfaces. *Biophysical Journal*, *278*, 1643–1654.

Pantaloni, D., Boujemaa, R., Didry, D., Gounon, P., & Carlier, M.-F. (2000). The Arp2/3 complex branches filament barbed ends: Functional antagonism with capping proteins. *Nature Cell Biology*, *2*, 385–391.

Pollard, T. D., & Borisy, G. G. (2003). Cellular motility driven by assembly and disassembly of actin filaments. *Cell*, *112*, 453–465.

Reymann, A.-C., Boujemaa-Paterski, R., Martiel, J.-L., Guérin, C., Cao, W., Chin, H. F., et al. (2012). Actin network architecture can determine myosin motor activity. *Science*, *336*, 1310–1314.

Reymann, A.-C., Martiel, J.-L., Cambier, T., Blanchoin, L., Boujemaa-Paterski, R., & Théry, M. (2010). Nucleation geometry governs ordered actin networks structures. *Nature Materials*, *9*, 827–833.

Reymann, A.-C., Suarez, C., Guerin, C., Martiel, J.-L., Staiger, C. J., Blanchoin, L., et al. (2011). Turnover of branched actin filament networks by stochastic fragmentation with ADF/cofilin. *Molecular Biology of the Cell*, *22*, 2541–2550.

Romero, S., Le Clainche, C., Didry, D., Egile, C., Pantaloni, D., & Carlier, M.-F. (2004). Formin is a processive motor that requires profilin to accelerate actin assembly and associated ATP hydrolysis. *Cell*, *119*, 419–429.

Sauer-Eriksson, A. E., Kleywegt, G. J., Uhlen, M., & Jones, T. A. (1995). Crystal structure of the C2 fragment of streptococcal protein G in complex with the Fc domain of human IgG. *Structure*, *3*, 265–278.

Schirenbeck, A., Bretschneider, T., Arasada, R., Schleicher, M., & Faix, J. (2005). The Diaphanous-related formin dDia2 is required for the formation and maintenance of filopodia. *Nature Cell Biology*, *7*, 619–625.

Steffen, A., Faix, J., Resch, G. P., Linkner, J., Wehland, J., Small, J. V., et al. (2006). Filopodia formation in the absence of functional WAVE- and Arp2/3-complexes. *Molecular Biology of the Cell*, *17*, 2581–2591.

Svitkina, T. M., & Borisy, G. C. (1999). Arp2/3 complex and actin depolymerizing factor/cofilin in dendritic organization and treadmilling of actin filament array in lamellipodia. *Journal of Cell Biology*, *145*, 1009–1026.

Svitkina, T. M., Bulanova, E. A., Chaga, O. Y., Vignjevic, D. M., Kojima, S., Vasiliev, J. M., et al. (2003). Mechanism of filopodia intitiation by reorganization of a dendritic network. *Journal of Cell Biology*, *160*, 409–421.

Takeya, R., Taniguchi, K., Narumiya, S., & Sumimoto, H. (2008). The mammalian formin FHOD1 is activated through phosphorylation by ROCK and mediates thrombin-induced stress fibre formation in endothelial cells. *EMBO Journal*, *27*, 618–628.

Urban, E., Jacob, S., Nemethova, M., Resch, G. P., & Small, J. V. (2010). Electron tomography reveals unbranched networks of actin filaments in lamellipodia. *Nature Cell Biology*, *12*, 429–435.

Vallotton, P., Gupton, S. L., Waterman-Storer, C. M., & Danuser, G. (2004). Simultaneous mapping of filamentous actin flow and turnover in migrating cells by quantitative fluorescent speckle microscopy. *Proceedings of the National Academy of Sciences of the United States of America*, *101*(26), 9660–9665.

Vicente-Manzanares, M., Ma, X., Adelstein, R. S., & Horwitz, A. R. (2009). Nonmuscle myosin II takes centre stage in cell adhesion and migration. *Nature Reviews Molecular Cell Biology*, *10*, 778–790.

Vignaud, T., Galland, R., Tseng, Q., Blanchoin, L., Colombelli, J., & Théry, M. (2012). Reprogramming cell shape with laser nano-patterning. *Journal of Cell Science*, *125*, 2134–2140.

Vignjevic, D., Yarar, D., Welch, M. D., Peloquin, J., Svitkina, T., & Borisy, G. G. (2003). Formation of filopodia-like bundles in vitro from a dendritic network. *Journal of Cell Biology*, *160*, 951–962.

Vinzenz, M., Nemethova, N., Schur, F., Mueller, J., Narita, A., Urban, E., et al. (2012). Actin branching in the initiation and maintenance of lamellipodia. *Journal of Cell Science*, *125*, 2775–2785.

Wagner, B., Tharmann, R., Haase, I., Fischer, M., & Bausch, A. R. (2006). Cytoskeletal polymer networks: The molecular structure of cross-linkers determines macroscopic properties. *Proceedings of the National Academy of Sciences of the United States of America*, *103*(38), 13974–13978.

Weichsel, J., Urban, E., Small, J. V., & Schwarz, U. S. (2012). Reconstructing the orientation distribution of actin filaments in the lamellipodium of migrating keratocytes from electron microscopy tomography data. *Cytometry. Part A*, *81A*, 496–507.

Wilson, C. A., Tsuchida, M. A., Allen, G. M., Barnhart, E. L., Applegate, K. T., Yam, P. T., et al. (2010). Myosin II contributes to cell-scale actin network treadmilling through network disassembly. *Nature*, *465*, 373–377.

Xu, K., Babcock, H. P., & Zhuang, X. (2012). Dual-objective STORM reveals three-dimensional filament organization in the actin cytoskeleton. *Nature Methods*, *9*, 185–188.

Yang, C., Czech, L., Gerboth, S., Kojima, S., Scita, G., & Svitkina, T. (2007). Novel roles of formin mDia2 in lamellipodia and filopodia formation in motile cells. *PLoS Biology*, *5*, 317.

Yang, C., & Svitkina, T. (2011). Filopodia initiation focus on the Arp2/3 complex and formins. *Cell Adhesion & Migration*, *5*, 402–408.